Molecular Pharmacology Fast Forward. Published on October 1, 2014 as DOI: 10.1124/mol.114.094862
This article has not been copyedited and formatted. The final version may differ from this version.

Characterization of Ritonavir-Mediated Inactivation of Cytochrome P450 3A4

Brooke M Rock, Shawna M Hengel, Dan A Rock, Larry C Wienkers and Kent L Kunze

Department of Pharmacokinetics and Drug Metabolism, Amgen, Inc, Seattle, WA (BMR, DAR, LCW)

Department of Medicinal Chemistry, University of Washington, Seattle, WA (SMH*, KLK)
* Current affiliation: Bioanalytical Development, Seattle Genetics, Bothell, WA 98011

Molecular Pharmacology Fast Forward. Published on October 1, 2014 as DOI: 10.1124/mol.114.094862
This article has not been copyedited and formatted. The final version may differ from this version.

Running Title Page

Running Title: Inactivation of CYP3A4 by Ritonavir

Address for Correspondence:

Brooke M Rock

1201 Amgen Court West

Seattle, WA 98119.

Ph: (206) 265-6109.

Fax: (206) 265-1149

E-mail: brooke@amgen.com.

Text pages: 29

Tables: 1

Figures: 7

Supplemental Figures: 4

References: 36

Abstract words: 248

Introduction words: 724

Discussion words: 1,522

Abbreviations: ACN, acetonitrile, CYP, cytochrome P450; DDIs, drug-drug interactions; HIV; human immunodeficiency virus; HLM, human liver microsomes; HPLC, high performance liquid chromatography; LC- MS/MS, liquid chromatography-tandem mass spectrometry; MBI, mechanism-based inactivation; MIC, metabolic-intermediate complex; RTV, ritonavir (1,3-thiazol-5-ylmethyl-*N*-[(2*S*,3*S*,5*S*)-3-hydroxy-5-[(2*S*)-3-methyl-2-{[methyl({[2-(propan-2-yl)-1,3-thiazol-4-yl]methy)carbamoyl]amino} butanamido]-1,6-diphenylhexan-2-yl]carbamate) and N-ritoniavr, Desthiazolylmethyloxycarbonyl ritonavir

Molecular Pharmacology Fast Forward. Published on October 1, 2014 as DOI: 10.1124/mol.114.094862
This article has not been copyedited and formatted. The final version may differ from this version.

Abstract

Ritonavir is a HIV protease inhibitor and an inhibitor of cytochrome P450 3A4 (CYP3A4), the major human hepatic drug-metabolizing enzyme. Given the potent inhibition of CYP3A4 by ritonavir, sub-therapeutic doses of ritonavir are utilized to increase plasma concentrations of other HIV drugs oxidized by CYP3A4, thereby extending their clinical efficacy. However, the mechanism of inhibition of CYP3A4 by ritonavir remains unclear. To date, data suggests multiple types of inhibition by ritonavir including mechanism-based inactivation by metabolic-intermediate complex formation, competitive inhibition, irreversible type II coordination to the heme iron and more recently heme destruction. The results presented here demonstrate that inhibition of CYP3A4 by ritonavir occurs by CYP3A4-mediated activation and subsequent formation of a covalent bond to the apoprotein. Incubations of [^{3}H]-ritonavir with reconstituted CYP3A4 and human liver microsomes resulted in a covalent binding stoichiometry equal to 0.93 ±0.04 moles of ritonavir bound per mole of inactivated CYP3A4. The metabolism of [^{3}H]-ritonavir by CYP3A4 leads to the formation of a covalent adduct specifically to CYP3A4, confirmed by radiometric LC-trace and whole protein mass spectrometry. Tryptic digestion of the CYP3A4-[^{3}H]-ritonavir incubations exhibited an adducted peptide (255-RM**K**ESRLEDTQKD-268) associated with a radiochromatic peak and a mass consistent with ritonavir plus 16 daltons, in agreement with the whole protein mass spectrometry. Additionally, nucleophilic trapping agents and scavengers of free oxygen species did not prevent inactivation of CYP3A4 by ritonavir. In conclusion, ritonavir exhibited potent time-dependent inactivation of CYP3A, with the mechanism of inactivation occurring though a covalent bond to Lys257 of the CYP3A4 apoprotein.

Molecular Pharmacology Fast Forward. Published on October 1, 2014 as DOI: 10.1124/mol.114.094862
This article has not been copyedited and formatted. The final version may differ from this version.

Introduction

Mechanism-based inactivation (MBI) of cytochrome P450 (CYP) enzymes represents several challenges for the development of therapeutics. Foremost, MBI has the potential to amplify the magnitude of a drug-drug interaction (DDI), by changing the clearance of co-administered drugs and ultimately, affecting patient safety (Fletcher et al., 2000; Miller et al., 2007; Fernandez-Montero et al., 2009). The MBI-mediated rate of inactivation relative to zero-order synthesis rate of new enzyme provides a path for estimating the magnitude of inhibition a MBI will have on drug disposition (Mayhew, 2000). However reactive metabolites, often the precursors to MBI, are less understood (Begriche et al., 2011) and predicting the impact of the reactive metabolites on safety is difficult. Therefore, it remains critical to understand the mechanism of bioactivation of CYP inhibitors to characterize the chemical entities that predispose MBI, which is challenging in part due to the diversity of CYP oxidative chemistry.

Ritonavir (Figure 1) is a rationally designed protease inhibitor for the treatment of human immunodeficiency virus (HIV) and a well-known inactivator of CYP3A (Koudriakova et al., 1998). Inactivation of intestinal and hepatic CYP3A during initial transit of the oral dose of ritonavir increases the bioavailability and decreases the rate of systemic elimination. These effects, in part, explain the high bioavailability and longer half-life of ritonavir, compared with other protease inhibitors (Koudriakova et al., 1998). Consequently, a standard HIV therapy combination makes use of an intentional DDI, where ritonavir is used to boost concentrations of other co-administered protease inhibitors by decreasing clearance via CYP3A inactivation. The dose of ritonavir administered in “boosted” protease inhibitor regimens is generally considered sub-therapeutic (100–200 mg) (Moyle and Back, 2001). The discovery that a low dose of ritonavir can be safely administered to enhance the effectiveness of other protease inhibitors has drastically reduced the adverse effects and improved the efficacy of treatment (Hirsch et al.,

Molecular Pharmacology Fast Forward. Published on October 1, 2014 as DOI: 10.1124/mol.114.094862
This article has not been copyedited and formatted. The final version may differ from this version.

2008). However, this pharmaco-enhancement effect does come with a cost because the safety and efficacy of numerous other medications metabolized by CYP3A is compromised.

The potent inhibitory effect on CYP3A4 by ritonavir has been demonstrated in *in vitro* preparations including expressed CYP3A4 enzyme, human enterocytes and human liver microsomes (HLMs) (Koudriakova et al., 1998). In general, CYP enzymes are inactivated by three distinct mechanisms: metabolic-intermediate (MI) complex formation (quasi-irreversible), covalent binding of a reactive intermediate to the apoprotein or direct alkylation of a reactive intermediate to the heme prosthetic group (Blobaum et al., 2002; Ortiz de Montellano, 2005). The structural complexity of ritonavir precludes the ready identification of the chemical moiety that undergoes bioactivation to an intermediate that would inactivate CYP3A. It has been proposed that ritonavir forms an MI complex with CYP3A4 (Ernest et al., 2005); however, the reactive metabolite(s) responsible for the formation of an MI complex or a proposed structure of the MI complex have not been reported. Additionally, it was demonstrated in one study that other protease inhibitors including amprenavir, nelfinavir and indinavir, are capable of forming MI complexes with CYP3A4 based on spectral evidence in CYP3A4 expressed enzymes (Ernest et al., 2005), however the authors were not able to generate MI complexes with ritonavir in HLMs, where CYP3A4 is the dominant CYP enzyme. Ritonavir is also reported to be a tight, irreversible binding inhibitor of CYP3A4 via coordination to the heme iron (Sevrioukova and Poulos, 2010). More recently, ritonavir has been reported to cause heme destruction in a reconstituted CYP3A4 system (Lin et al., 2013). Together, these reports suggest that multiple mechanisms of bioactivation and inhibition may occur with ritonavir and CYP3A4.

Although the mechanism of inactivation of CYP3A4 by ritonavir is unclear, the CYP-mediated metabolism of ritonavir has been characterized (Kumar et al., 1996; Denissen et al., 1997). The metabolism of ritonavir in HLMs leads to the formation three major metabolites. M1 (N-ritonavir, Figure 1) is formed by the CYP3A4-mediated cleavage of the 2-(1-methylethyl)

Molecular Pharmacology Fast Forward. Published on October 1, 2014 as DOI: 10.1124/mol.114.094862
This article has not been copyedited and formatted. The final version may differ from this version.

thiazolylmethyl group to form a primary amine. A possible route for MI complex formation is via further metabolism of this primary amine, based on numerous reports of the ability of substituted aliphatic amines to form MI complexes with CYP enzymes under turnover conditions (Bensoussan et al., 1995; Ortiz de Montellano, 2005).

The postulated formation of an MI complex may not be the only viable mechanism for inactivation of CYP3A4 by ritonavir, especially considering formation of the MI complex only accounts for 64% of the inactivated CYP3A4 (Ernest et al., 2005). Inhibition studies using M1 or any metabolite of ritonavir have not been reported, although there is data demonstrating that metabolites of ritonavir (generated *in situ*) added to a secondary incubation had no effect on the rate of metabolism of ritonavir by intact microsomes (Koudriakova et al., 1998). Additionally, comparison of the ability of ritonavir and structural analogs to inactivate the enzyme showed that the potent inhibitory properties of ritonavir require the presence of both the 2'-isopropyl-thiazolyl and 2-(1-methylethyl)thiazolyl groups (Kempf et al., 1997). The aim of this work is to further characterize the mechanism(s) of CYP3A4 inactivation by ritonavir by evaluating, MI complex formation, heme-adduct formation, and irreversible covalent binding to CYP3A4.

Molecular Pharmacology Fast Forward. Published on October 1, 2014 as DOI: 10.1124/mol.114.094862
This article has not been copyedited and formatted. The final version may differ from this version.

Materials and Methods

Materials

All commercial solvents (Sigma-Aldrich) were of analytical grade with the exception of solvents used with the Waters Acquity Ultra Performance Liquid Chromatography (UPLC), which were LC/MS Optima® grade. CYP 3A4 Supersomes™ were purchased from BD Biosciences (Franklin Lakes, NJ). CYP 3A4 was co-expressed with cytochrome b_5 and cytochrome CYP reductase. Human CYP 3A4 was expressed and purified as described previously (Baer et al., 2007). The pCW 3A4-His6 expression vector and C41(DE3) cells were kindly provided by Dr. William Atkins (University of Washington, Seattle, WA). Rat CYP reductase was expressed and purified as described previously (Shen et al., 1989). The expression vectors encoding rat CYP reductase and BL21(DE3) and purified rat cytochrome b_5 were kindly provided by Dr. Allan Rettie (University of Washington, Seattle, WA). Ritonavir, d_6-ritonavir and desthiazolylmethyloxycarbonyl ritonavir were purchased from Medical Isotopes, Inc. (Pelham, NH). [^{3}H]-ritonavir was purchased from Moravek Biochemicals (Brea, CA), the specific activity was 78 GBq/mmol. Midazolam and d_4-1'-hydroxylmidazolam were purchased from Cerillant® (Round Rock, TX). Sequencing-grade trypsin and proteinase K was purchased from Roche (Indianapolis, IN). Human liver microsomal preparations (lot #144, 160 and 169), with known CYP 3A content, were obtained through the University of Washington Medical Center Liver Bank (Seattle, WA). All other chemicals were purchased from Sigma-Aldrich, unless specified.

CYP 3A4 activity assay

The turnover of midazolam to 1'-OH midazolam was used to probe the activity of CYP 3A4. The general incubation conditions were midazolam (1 µM), CYP 3A4 enzyme (0.1 µM) and 1 mM NADPH in 0.1 M potassium phosphate buffer (pH 7.4) in a total volume of 200 µL. After three minutes, incubations were quenched by addition of an equal volume of ACN containing 0.5 µM

Molecular Pharmacology Fast Forward. Published on October 1, 2014 as DOI: 10.1124/mol.114.094862
This article has not been copyedited and formatted. The final version may differ from this version.

of d_4-1'-OH midazolam as an internal standard. After centrifugation at 13,000 xg for 10 minutes, the supernatants were injected onto a Waters Acquity UPLC C_{18} BEH (2.1 x 50 mm, 1.7 microns particle size) column attached to a Waters ACQUITY Ultra Performance LC™ System. The UPLC was in line with a Waters Micromass® Premier™ XE (Waters Corp., Milford, MA), a tandem quadrupole mass spectrometer, operated in positive ion mode. The precursor > fragment ions monitored were 1'-OH midazolam (342 > 324 *m/z*) and 1'-OH-d_4 midazolam (346 > 328 *m/z*). The peaks eluted using a linear gradient at 0.3 mL/minutes and mobile phases A: 0.1% formic acid in water and B: 0.1% formic acid in acetonitrile. The gradient started at 90% A (0-0.5 minutes). Solvent B was linearly increased from 10% at 0.5 minutes to 100% at 3 minutes. The total run time was 4 minutes. The cone and collision energies were 25 V and 15 kV respectively, for both channels.

CYP 3A4 inactivation assay

CYP3A4 Supersomes™ (0.1 µM) in 0.1 M potassium phosphate buffer (pH 7.4) were warmed in to 37ºC in the presence of varying concentrations of ritonavir or N-ritonavir (0-10 uM; final concentration) for 3 minutes. Ritonavir or N-ritonavir was added to the incubations in methanol, not to exceed 0.5% of total incubation volume. The pre-incubation assay, set up in a 96-well plate format, was initiated with the addition of NADPH (10 mM, 0.02 mL). At pre-incubation time points of 0.25, 0.5, 1, 2, 3, 4 and 8 minutes, 10 µL of the pre-incubation assay was transferred into a CYP3A4 midazolam activity assay. Ritonavir is a potent reversible inhibitor of CYP3A4 (IC_{50}= 0.05 uM, (Ernest et al., 2005)); therefore, 1:100 dilutions were made into the activity assay to minimize the effect of competitive inhibition of midazolam hydroxylation in the activity assay. After three min, the activity assay was quenched with an equal volume ACN containing 0.5 µM of internal standard (1'-OH midazolam-d_4). The 96-well plate was centrifuged at 2500 rpm for 10 minutes and 0.05 mL was transferred into a new 96-well plate for liquid chromatography tandem mass spectrometry (LC/MS/MS) analysis. All experiments were

Molecular Pharmacology Fast Forward. Published on October 1, 2014 as DOI: 10.1124/mol.114.094862
This article has not been copyedited and formatted. The final version may differ from this version.

performed in triplicate. The same experimental setup described above was used to measure CYP3A4 inactivation in reconstituted 3A4 (incubation conditions described below in *CO difference spectral analysis*) to establish the inactivation profile was the same in each system. Additionally, the rate of inactivation of CYP 3A4 Supersomes™ by ritonavir (1.5 μM) was determined in the presence of the following nucleophilic trapping agents: L-glutathione (1 mM), N-acetyl cysteine (1 mM), N-acetyl lysine (1 mM) and potassium cyanide (0.5 mM).

Rates of enzyme inactivation (k_{obs}) were estimated from the slopes of the semi-log plots of percent remaining enzyme activity in the presence and absence of inactivator with time. Kinetic parameters for enzyme inactivation were obtained by nonlinear regression without weighting using Sigma Plot 9.0 (Systat Software, Inc., San Jose, CA) where k_{obs} is related to the inhibitor concentration (I) according to the following equation:

$$k_{obs} = \frac{k_{inact} \times [I]}{K_I + [I]}$$

where k_{inact} is the maximal inactivation rate constant and K_I is the inhibitor concentration that produces a k_{obs} that is half k_{inact}. This equation assumes that the loss of enzyme is due solely to inactivation by the inhibitor, and that there is negligible change in the inhibitor concentration throughout the incubation; therefore, preliminary experiments were performed to determine appropriate concentrations of enzyme and inhibitor to use in order to avoid depletion.

Metabolic-intermediate complex formation

CYP 3A4 Supersomes™ or HLMs were used to characterize MI complex formation associated with the metabolism of ritonavir, N-ritonavir and a positive control, troleandomycin. The formation of an MI complex was monitored on an Aminco DW-2 spectrophotometer (Olis, Bogart, GA) by repetitively scanning from 430-495 nm over 30 minutes. Sample and reference

Molecular Pharmacology Fast Forward. Published on October 1, 2014 as DOI: 10.1124/mol.114.094862
This article has not been copyedited and formatted. The final version may differ from this version.

cuvettes contained CYP 3A4 (0.1 µM) or HLMs (0.5 mg/mL), 0.1 M potassium phosphate buffer (pH 7.4) and 10 µM inhibitor to a total volume of 0.45 mL. After three minutes of pre-incubation at 37 °C, NADPH (10 mM, 0.05 mL) and potassium phosphate buffer (0.1 M, 0.05 mL) were added to the sample and reference cuvettes, respectively. The concentration of MI complex formation was estimated using an extinction coefficient of 65 mM^{-1} cm^{-1} for the absorbance difference between 490 and 455 nm (Liu and Franklin, 1985). To validate the spectral evidence of MI complex formation, 1 mM potassium ferricyanide ($K_3[Fe(CN)_6]$) was added to sample and reference cuvettes after 30 minutes and an additional scan was taken. Additionally, the reversal of MI complex by $K_3[Fe(CN)_6]$ was confirmed using the midazolam-CYP 3A4 activity assay. These experiments consisted of three sequential incubations: primary 0 or 30 minutes incubations with or without inhibitors (ritonavir, N-ritonavir or troleodomyacin), secondary 5 minutes incubations of the primary incubation mixtures with or without 1 mM $K_3[Fe(CN)_6]$ and tertiary 3 minutes incubations of the secondary incubation mixtures with midazolam. The primary incubation solutions, containing CYP 3A4 (0.1 µM) or HLMs (0.5 mg/mL), 0.1 M potassium phosphate buffer (pH 7.4) and 10 µM inhibitor to a total volume of 0.18 mL. The primary incubation reactions were initiated by the addition of 20 µL of a 10 mM solution of NADPH. After a 0 or 30 minutes primary incubation at 37°C, 50 µL of each primary incubation mixture was added to 100 µL of the secondary incubation solutions containing 0.1 M potassium phosphate buffer (pH 7.4) with or without 1 mM $K_3[Fe(CN)_6]$ and incubated for 5 minutes. After a 5 minutes secondary incubation at 37°C, each secondary reaction mixture was diluted 5-fold with the tertiary incubation solutions, which contained 0.1 M potassium phosphate (pH 7.4) buffer, 1 µM midazolam and 1.0 mM NADPH and then were incubated for 3 minutes. At the end of the tertiary incubation reactions, each tertiary reaction mixture was quenched with 100 µL of acetonitrile containing 1'-OH midazolam-d_4 (0.5 µM) as an internal standard. The percentage of metabolic activity was calculated for each sample after a 0 or 30 minutes pre-incubation with

Molecular Pharmacology Fast Forward. Published on October 1, 2014 as DOI: 10.1124/mol.114.094862
This article has not been copyedited and formatted. The final version may differ from this version.

each inhibitor and compared with each control sample without inhibitor as well as in the presence and absence of $K_3[Fe(CN)_6]$ as previously reported (Takakusa et al., 2011).

Partition Ratio

Ritonavir or N-ritonavir (0-20 μM, final concentration) was incubated with 0.11 μM of CYP 3A4 Supersomes™ in 0.1 M potassium phosphate buffer to a total volume of 0.18 mL. The reactions were initiated by the addition of NADPH (10 mM, 0.02 mL) and incubated at 37 ºC for 30 minutes. Reactions were run in triplicate and aliquots were removed for measurement of CYP 3A4 activity by 1'-OH midazolam formation, as described above. The percent remaining CYP 3A4 activity at each substrate concentration was determined by dividing control well values by the 30 minutes time point values. The partition ratios were estimated from the intercept of the linear regression line for the lower ratios of inhibitor to CYP 3A4 and the straight line obtained from the higher ratios of inhibitor to CYP 3A4 as previously described (Silverman, 1988).

CO difference spectral analysis

Purified CYP 3A4 was reconstituted with 60 μg of a (1:1:1) mixture of L-α-dilauroyl-phosphocholine, L-α-dioleyl-sn-glycero-3-phosphcholine, and L-α-phosphatidylserine, 200 μg of sodium cholate, 100 U catalase, 2mM glutathione in a 1 molar ratio of CYP 3A4 to CYP reductase and 0.5 molar ratio of CYP 3A4 to cytochrome b_5. This mixture was transfered into buffer containing 50 mM HEPES (pH 7.4), 20% glycerol, 30 mM $MgCl_2$, and 0.5 mM EDTA to a total volume of 1 mL, as previously described(Shaw et al., 1997). Ritonavir or 1-aminobenzotriazole (10 μM) was incubated with the reconstituted CYP 3A4 mixture (0.05 μM) in the presence and absence of NADPH at 37ºC for 30 minutes. The reaction mixture was split into a reference and sample cuvette to determine CYP content by CO difference spectra. The reduced CO difference spectrum was determined by first reducing the enzyme, in both the reference and sample cuvettes, with sodium dithionite and obtaining a baseline spectrum by

Molecular Pharmacology Fast Forward. Published on October 1, 2014 as DOI: 10.1124/mol.114.094862
This article has not been copyedited and formatted. The final version may differ from this version.

scanning from 400-500 nm on an Aminco DW-2 spectrophotometer (Olis, Bogart, GA). The sample cuvette was then bubbled with CO for approximately 1 minute, and the spectrum was acquired. At the end of 30 minutes an aliquot was removed and CYP3A4 activity was measured.

Trapping of reactive intermediates with nucleophilic reagents

The following nucleophilic trapping agents, L-glutathione (1 mM), N-acetyl cysteine (1 mM), N-acetyl lysine (1 mM) and potassium cyanide (0.5 mM), were incubated with CYP 3A4 Supersomes™ (0.1 µM), ritonavir (1.5 µM) or [^{3}H]ritonavir (1.5 µM) in 0.1 M potassium phosphate (pH 7.4) buffer in a total volume of 0.2 mL for 30 minutes. Control incubations were run in parallel in the absence of NADPH and/or absence of the trapping reagents. Aliquots of the incubations were analyzed for ritonavir metabolites and potential adducts to trapping agents by LC/MS. All LC/MS experiments were performed on a LTQ Orbitrap Velos mass spectrometer (Thermo Fisher Scientific, San Jose, CA) coupled to an Accela 1250 HPLC system with a Leap CTC PAL autosampler (Leap Technologies, Carrboro, NC). Briefly, the following three methods were employed to search for putative adducts: (1) LC-radiochromatography in-line with mass spectroscopy; (2) Q1 scanning and single ion monitoring for predicted masses of adducts; (3) MRM triggering on neutral loss of 129 for glutathione adducts.

[^{3}H]-ritonavir binding stoichiometry

[^{3}H]-ritonavir (1.5 µM) was incubated with CYP 3A4 Supersomes™ (0.1 µM) or HLMs (0.5 mg/mL) (lot# 144, 160 or 169) in 0.1 M potassium phosphate (pH 7.4) buffer in a total volume of 0.2 mL for 30 minutes in the presence and absence of 1 mM NADPH. Aliquots (150 µL) of the samples were mixed (1:1 v/v) with 10 mg/mL of bovine serum albumin and the protein was precipitated by adding a 5-fold volume of a 5% solution of sulfuric acid in methanol. The precipitates were collected by centrifugation, and the resulting pellets were washed six times with buffer (100 mM potassium phosphate, pH= 7.4) until the radioactivity in the supernatant

Molecular Pharmacology Fast Forward. Published on October 1, 2014 as DOI: 10.1124/mol.114.094862
This article has not been copyedited and formatted. The final version may differ from this version.

was essentially at background level (< 20 dpm). The final pellets were dissolved in 1 M NaOH, incubated at 60ºC for 2 hours and neutralized with HCl prior to liquid scintillation counting using Econo-Safe counting cocktail (Research Products International Corp., Mt. Prospect, IL) on a Packard Tricarb 1600TR liquid scintillation analyzer (Downers Grove, IL).

Covalent binding of [^{3}H]-ritonavir by HPLC

Reaction mixtures containing reconstituted CYP 3A4 (0.1 µM), as described above, and [^{3}H]-ritonavir (1.5 µM) were incubated for 30 minutes in the presence and the absence of NADPH. The control (-NADPH) and inactivated (+NADPH) samples (pellets) were washed six times with 2X volume of ammonium bicarbonate buffer (100 mM, pH 8) and concentrated using a Centricon® concentrator (Millipore, Billerica, MA). The recovery from the filtration was greater than 85%, based on radioactivity counts before and after concentration. A 25 µL sample was then analyzed by HPLC (Hewlett Packard 1100 series, Waldbronn, Germany) on a C_4 protein and peptide column (4.6 x 250 mm, 300 Å, VYDAC, Hesperia, CA) with a solvent system consisting of solvent A (0.1% TFA in water) and solvent B (0.1% TFA in ACN). A linear gradient was used to separate the heme, CYP reductase, cytochrome b_5 and CYP 3A4. The gradient started at 30% B and increased linearly to 85% B over 25 minutes with a flow rate of 0.5 mL/min. The column was washed for 5 minutes at 90% B, and equilibrated for 5 minutes at initial starting conditions for a total run time of 35 minutes. An Agilent 1100 DAD detector was set at 280 nm for detection of proteins and at 405 nm for detection of heme. Fractions from the HPLC eluent were collected every 30 seconds and the radioactivity was determined by liquid scintillation counting, using Econo-Safe counting cocktail (Research Products International Corp., Mt. Prospect, IL) on a Packard Tricarb 1600TR liquid scintillation analyzer (Downers Grove, IL).

Molecular Pharmacology Fast Forward. Published on October 1, 2014 as DOI: 10.1124/mol.114.094862
This article has not been copyedited and formatted. The final version may differ from this version.

Whole protein mass spectral analysis of CYP3A4

Ritonavir (10 µM) was incubated with CYP 3A4 Supersomes™ (0.1 µM) or reconsitutued CYP 3A4 (0.5 µM) in 0.1 M potassium phosphate (pH 7.4) buffer in a total volume of 0.2 mL in the presence and absence of 1 mM NADPH. The incubation was allowed to proceed for 10 minutes, at which point a 100 µL aliquot was transferred to a Microcon centrifugal filter tube (30-kDa filter) and centrifuged for 5 minutes at 10,000 rpm. The sample was analyzed by on a LTQ Orbitrap Velos mass spectrometer (Thermo Fisher Scientific, San Jose, CA) coupled to an Accela 1250 HPLC system with a Leap CTC PAL autosampler (Leap Technologies, Carrboro, NC). Initial HPLC conditions were 82% solvent A (0.05% TFA in H_2O) and 18% solvent B (0.05% TFA in acetonitrile) at a flow rate of 250 µL/min. The following linear gradient elution profile was utilized: 18% B for 1 minutes, 18-90% solvent B in 12 minutes, 90% solvent B for 2 minutes separated on a Biobasics4 column (Thermo Fisher Scientific, San Jose, CA). LTQ Orbitrap parameters were set as follows: source temperature, 350°C; sheath gas, 35 arbitrary units; auxiliary gas, 5 arbitrary units; spray voltage,3 kV; capillary temperature, 300°C; S-lens radiofrequency, 85%; resolution, 15,000; ion trap and Orbitrap maximum injection time, 500 ms; *m/z* scan range, 650 to 1850. Mass spectra were averaged over the entire width of the peak and deconvoluted using ProMass 2.0 software (Novatia, Monmouth Junction, NJ). Each sample was run in triplicate to determine the standard deviation of the deconvulated mass.

Proteolytic digestion of CYP 3A4

Reaction mixtures with reconstituted CYP 3A4 (0.1 µM), as described above, and [^{3}H]-ritonavir or ritonavir (10 µM) were incubated for 10 minutes in the presence and absence of NADPH. The incubations were placed on ice and aliquots of 100-200 µL were concentrated by a SpeedVac to a final volume of 15 µL. To each sample, 800 µL of 50 mM ammonium bicarbonate buffer (pH 8.1) and 100 µL of methanol were added. The mixtures were then incubated with sequence

Molecular Pharmacology Fast Forward. Published on October 1, 2014 as DOI: 10.1124/mol.114.094862
This article has not been copyedited and formatted. The final version may differ from this version.

grade trypsin or proteinase K (Roche, Indianapolis, IN) in a 1:50 (w/w) ratio for 12 hours at room temperature. The pH was adjusted to 5 with 0.1% TFA and 100 µL of ACN was added to final of 1 mL. Samples were desalted using a standard solid phase extraction protocol (SPE) with a Vydac silica C_{18} macrospin column (The Nest Group, Southborough, MA). Eluate was concentrated by SpeedVac to a volume of 20 µL and frozen at -80ºC until mass spectral analysis.

Mass Spectral Analysis of CYP 3A4 Peptides

The peptides resulting from digests, described above, of CYP 3A4 and [^{3}H]-ritonavir were injected onto Jupiter 3u, 4.6x150 mm C18 column (Phenomenex, Torrance, CA) at a flow rate of 500 µL/min with 100 µL/min diverted into MS and 400 µL/min diverted to a liquid chromatography-accurate radioisotope counting system (LC-ARC™, AIM Research Company, Hochessin, DE) operated in dynamic flow mode (flow cell volume 250 µL). Initial conditions were 98% solvent A (0.05% formic acid in H_2O) and 2% solvent B (0.05% formic acid in acetonitrile), and the following linear gradient was used to elude the peptides: 2% B for 2 minutes, 2-95% B in 35 minutes, and 95% B for 5 minutes with an Accela 1250 HPLC system coupled to a Leap CTC PAL autosampler (Leap Technologies, Carrboro, NC), which was interfaced with a linear ion trap (LTQ) – Orbitrap (OT) Velos mass spectrometer (Thermo Fisher Scientific, San Jose, CA). All ions were measured in positive ion mode; precursor masses were acquired in the OT, while the top five most intense multiply charged ions in each MS spectrum were selected for fragmentation in the LTQ. Fragment ion spectra acquired from collision induced dissociation (CID) were produced using 35% collision energy and a 1.0 Da isolation window. The resulting data was searched via SEQUEST (Yates et al., 1995) embedded in Proteome Discoverer 1.2 (Thermo Scientific, San Jose, CA). All positive modification identifications were manually validated and assessed based on mass accuracy specifications. The modified peptides were also identified based on LC-radiometric trace.

Molecular Pharmacology Fast Forward. Published on October 1, 2014 as DOI: 10.1124/mol.114.094862
This article has not been copyedited and formatted. The final version may differ from this version.

Results

Time-dependent inactivation of CYP 3A4 by ritonavir and metabolite, N-ritonavir

Ritonavir and a primary metabolite, N-ritonavir (Figure 1) were determined to be a potent, time-dependent inactivator of CYP 3A4 with a K_I= 0.59 and 1.4 μM and k_{inact}= 0.53 and 0.33 min^{-1}, respectively (Table 1). A substrate depletion-based partition ratio was determined for both inhibitors. The percentage of CYP 3A4 activity remaining at 10 minutes was plotted as a function of the molar ratio of inhibitor to CYP 3A4. The turnover number was estimated from the intercept of the lower linear ratios of inhibitor to CYP 3A4 with the line derived from the higher ratios of inhibitor to CYP 3A4 (data not shown). By this method, the turnover number minus one is equal to the substrate-based depletion partition ratio (Silverman, 1988). Partition ratio estimates for ritonavir and N-ritonavir was 19 ± 3 and 12 ± 2, respectively (Table 1). The inactivation rate of ritonavir was also determined in the presence of four nucleophilic trapping agents (0.5 mM KCN, 1 mM N-acetyl cysteine, 1 mM N-acetyl lysine and 1 mM L-glutathione). In each case, the rate of inactivation was not altered by inclusion of the trapping reagents (Supplemental Figure 4). Additionally, co-incubations with the nucleophilic trapping agents (e.g. KCN, GSH) and [^{3}H]-ritonavir did not indicate the formation of any adducts to ritonavir both from LC/MS analysis and LC-radiometric traces.

CYP 3A4 MI complex formation

Spectrophotometric absorbance difference spectra of CYP 3A4 Supersomes™ and HLMs were collected between 430 and 490 nm in the presence of ritonavir, N-ritonavir or troleandomycin in order to determine if MI complexes were formed with the prosthetic heme (Figure 2). No MI complex was observed with ritonavir; however, an MI complex was observed with N-ritonavir and a positive control, troleandomycin. Treatment of an MI complex with 1 mM ferricyanide ($K_3[Fe(CN)_6]$) has been shown to oxidize the coordinating nitroso ligand of an MI

Molecular Pharmacology Fast Forward. Published on October 1, 2014 as DOI: 10.1124/mol.114.094862
This article has not been copyedited and formatted. The final version may differ from this version.

complex, leading to a loss of the peak at 455 nm and a restoration of catalytic activity (Schenkman et al., 1972). Thus, experiments with subsequent $K_3[Fe(CN)_6]$ addition followed by activity measurements were performed with CYP 3A4 in the presence of ritonavir as well as N-ritonavir and troleandomycin (Delaforge et al., 1984) (Figure 2). As expected, the addition of 1 mM $K_3[Fe(CN)_6]$ regenerated the activity of CYP 3A4 in the N-ritonavir and troleandomycin incubations. However, the activity of CYP 3A4 was not restored in the case of ritonavir. Under co-incubation condition with equal molar amounts of ritonavir and N-ritonavir, no formation of an MI complex was observed (Figure 2). Together, these findings demonstrate that an inactivating MI complex is not formed by CYP 3A4 metabolism of ritonavir.

CYP 3A4 CO binding

The observation that metabolism of ritonavir does not lead to the formation an MI complex with CYP 3A4, but does lead to enzyme inactivation, led to the consideration that ritonavir is metabolized to a reactive intermediate that is capable of forming a covalent bond to prosthetic heme of CYP 3A4. A CO-binding experiment was performed to explore this possibility, given that alkylated prosthetic heme will not form a characteristic CYP CO-difference spectrum. The spectral experiments with reconstituted CYP 3A4 revealed no significant difference in the 450 nm absorbance between the control sample (-NADPH) and the sample treated with ritonavir and NADPH (Figure 3). This result, in addition to no radioactivity bound to the heme iron (Figure 4), demonstrate that a heme adduct is not formed during enzyme inactivation by ritonavir.

Covalent binding to CYP 3A4 by ritonavir

CYP 3A4 Supersomes™ and three lots of HLMs with varying CYP 3A concentrations were exposed to [^{3}H]-ritonavir in the absence and presence of NADPH to test for covalent binding to microsomal protein (Figure 5). Residual noncovalently bound [^{3}H]-ritonavir was

Molecular Pharmacology Fast Forward. Published on October 1, 2014 as DOI: 10.1124/mol.114.094862
This article has not been copyedited and formatted. The final version may differ from this version.

separated from protein by extensive washing of the precipitated protein mixture. To ensure all of the noncovalently bound [^{3}H]-ritonavir was removed; the washes were continued until the radiometric counts reached background levels. In each case, there was a NADPH-dependent incorporation of [^{3}H]-ritonavir-derived radioactivity to the denatured protein fraction. The amount of CYP 3A was positively correlated with the amount of radiolabel covalently bound to total protein (r^2 =0.93, Figure 5). The stoichiometry was also determined based on CYP 3A content. For example, in CYP 3A4 Supersomes™, 8.7 pmoles of radiolabel equivalents were found bound to total protein in an incubation that contained 10 pmoles of CYP 3A4. In the case of the three lots of HLMs, the binding stoichiometry was 0.87, 0.85 and 0.91, respectively. These results demonstrate that CYP 3A4 is the major target for the binding of bioactivated ritonavir. To further investigate the covalent binding of ritonavir to CYP 3A4 apoprotein, reconstituted CYP 3A4 with rat cytochrome CYP reductase and rat cytochrome b_5 was incubated with [^{3}H]-ritonavir and analyzed by UV/LC-radiometric detection. The elution profile of the reconsitituted enzyme system was monitored at 405 and 280 nm to detect free heme and proteins, respectively. Heme had a retention time of 18 minutes and can be observed in the LC trace of Figure 4. The retention times for cytochrome b_5, CYP reductase and CYP 3A4 were 24, 26 and 28 minutes, respectively. Several radioactive peaks were found in the NADPH-treated samples with no detectable radioactivity in the control sample (-NADPH). [^{3}H]-ritonavir associated radioactivity was mainly localized to the CYP 3A4 apoprotein containing fractions in the inactivated samples. In agreement with the CO-binding study, there was no radioactivity associated with the heme peak of CYP 3A4. Based on the known specific activity of [^{3}H]-ritonavir and a calculation of the amount of CYP 3A4 injected onto the column, a binding stoichiometry of 0.91 ±0.05 was calculated which is in agreement with total precipitated protein binding studies. Overall, these results show that most of the binding of bioactivated [^{3}H]-ritonavir to precipitated proteins is localized to CYP 3A4 apoprotein.

Molecular Pharmacology Fast Forward. Published on October 1, 2014 as DOI: 10.1124/mol.114.094862
This article has not been copyedited and formatted. The final version may differ from this version.

Characterization of CYP apoprotein adduct by ritonavir

Whole protein mass spectrometry was used to determine the molecular mass of the adducted CYP 3A4 protein with ritonavir and d_6-ritonavir. The two control samples (minus NADPH and minus ritonavir) yielded a deconvoluted envelope mass envelope of 56,259 Da, which corresponds to CYP 3A4 apoprotein. In the plus NADPH sample, a CYP 3A4 apoprotein adduct was observed with a mass of 737 Da and 743 Da, respectively for ritonavir and d_6-ritonavir, indicative of the addition of ritonavir plus 16 amu to CYP 3A4 protein (Figure 6).

A fraction of the incubation used for whole protein mass spectral analysis was subjected to tryptic and proteinase K digestion to identify the specific amino acid adducted by bioactivated ritonavir. Incubations with [^{3}H]-ritonavir were also subjected to tryptic and proteinase K digestion which enabled quantitation of [^{3}H]-ritonavir bound to peptides via LC-radiochromatography. The radiochromatograph of the tryptic digests revealed a single peak at 21.5 minutes (Supplemental Figure 1). The counts associated with this peak were calculated to be 87% of the total CYP 3A content, in alignment with the precipitated protein binding studies (Figure 5). Conversely, radiochromatograph of the proteinase K digests did not reveal any radioactive peaks. LC/MSMS data for both digests were acquired using an LTQ-OT, and data was searched using SEQUEST From the tryptic digest dataset, CYP 3A4 was identified with 74 % sequence coverage. The analyses revealed that Lys257 was the adducted amino acid in the modified peptide sequence of 255-RM**K**ESRLEDTQKHR-268. The observed doubly charged precurosor ion was within 12.3 ppm of the theoretical values, and all annotated fragment ions were within 8 ppm (Figure 7). The identity of the modified peptide was further characterized by manual inspection of the MS/MS spectra. For example, an ion (m/z 749.12) corresponded to the loss of ritonavir plus the nitrogen from the adducted lysine residue on the peptide (Figure 7), further confirming the site of modification. In the controls, minus NADPH or minus ritonavir, the adducted peptide was not observed.

Molecular Pharmacology Fast Forward. Published on October 1, 2014 as DOI: 10.1124/mol.114.094862
This article has not been copyedited and formatted. The final version may differ from this version.

From the data of the proteinase K digest CYP 3A4 was identified with 89% sequence coverage. Based on the lack of a radioactive peptide peak in the proteinase K digests, the stability of ritonavir under proteinase K digestion conditions was evaluated. Ritonavir is cleaved into two fragments under the digestion conditions (Supplemental Figure 2). The lack of stability of ritonavir under the digestion conditions also explains the loss of radioactivity from the adducted peptide. Knowledge of this unique cleavage allowed different modifications of CYP 3A4 by ritonavir to be searched for in the data. This revealed a similar adducted peptide (255-RMK*E-258, observed within 13.4 ppm of the theoretical value) to the same amino acid (Lys257) as was observed in the tryptic digest (Supplemental Figure 3). The MS/MS data also confirmed the adduct localization on the isopropyl-end of ritonavir, with all assigned fragment ions within 5 ppm of the theoretical values. In the control data, (minus NADPH or minus ritonavir) the adducted peptide was not observed.

Molecular Pharmacology Fast Forward. Published on October 1, 2014 as DOI: 10.1124/mol.114.094862
This article has not been copyedited and formatted. The final version may differ from this version.

Discussion

The potent inhibitory effect on CYP3A4 by ritonavir has been demonstrated across *in vitro* preparations including expressed CYP3A4 enzyme (Supersomes™), purified, reconstituted 3A enzyme, human enterocytes and human liver microsomes (Kumar et al., 1996; Koudriakova et al., 1998; Ernest et al., 2005). Additionally, the therapeutic use of ritonavir as a "booster" for other HIV protease inhibitors demonstrates that ritonavir is also an effective *in vivo* CYP3A4 inhibitor (Kempf et al., 1997). However, the mechanism(s) that are responsible for the inactivation of CYP3A4 by ritonavir remain unknown. The structural complexity of ritonavir precludes the identification a potential chemical moiety for bioactivation. Given the diversity of CYP-mediated bioactivation reactions, it is common for competing mechanisms of inhibition to occur. For example, 17-α-ethynylestradiol inactivates CYP3A by both heme modification and covalent binding to the protein (Lin and Hollenberg, 2007). The three possible routes of CYP3A4 inactivation (MI complex formation, heme modification and apoprotein adduction) were investigated to elucidate the mechanism of ritonavir mediated CYP3A4 inactivation.

A previous report proposed that ritonavir inactivated CYP3A4 via the formation of an MI complex with rapid loss of enzyme activity (Ernest et al., 2005) (K_I= 0.59 μM; k_{inact}= 0.53 min^{-1}). Therefore, the precursor to inactivation must arise from multiple oxidative reactions with ritonavir and is likely a result of sequential metabolism. Converse to these results, in this study no MI complex was observed with ritonavir and CYP3A4; whereas, under similar conditions an MI complex was observed with the positive control troleandomycin. In addition, ferricyanide reversed the MI complex with troleandomycin, however activity was not restored with ritonavir. The discrepancy in the ability to observe MI complex formation could be related to experimental design including ritonavir concentration, analytical techniques or complexities of sequential metabolism kinetics.

Molecular Pharmacology Fast Forward. Published on October 1, 2014 as DOI: 10.1124/mol.114.094862
This article has not been copyedited and formatted. The final version may differ from this version.

Heme modification is a common mechanism for CYP3A4 inactivation from terminal alkyne, aldehyde and furan functional groups (Ortiz de Montellano and Kunze, 1981; Kunze et al., 1983; Ortiz de Montellano, 2005). Ritonavir does not contain any of the aforementioned moieties; however, heterocyclic rings have demonstrated the ability to ring open and inactivate CYP enzymes. Ritonavir-mediated inactivation through heme modification was explored. No evidence for the formation of a heme adduct either by CO binding or LC/radiometric detection was observed when ritonavir was incubated with CYP3A4 Supersomes™ or with purified CYP3A4 reconstituted with CYP reductase and cytochrome b_5. The integrity of the CYP3A4 heme chromophore after incubations with ritonavir suggest that inactivation occurs through a mechanism independent of heme destruction. This is contrary to the recent report by Lin et. al (Lin et al., 2013) where the authors found that ritonavir inactivation of CYP3A4 was due to heme destruction with the formation of a heme-protein adduct, and no significant modification of the apoprotein. The report of heme destruction and a heme-protein adduct were performed with reconstituted CYP3A4 and CYP reductase, in comparison to the studies performed here in both CYP 3A4 Supersomes™ and reconstituted 3A4 enzyme with reductase and cytochrome b_5. More so, Lin et al. report the formation of glutathione adducts which were not observed in our studies. The difference in ritonavir metabolism and the role that cytochrome b_5 may play in the activation of ritonavir (and possibly other CYP3A4 substrates) is worthy of further research. However, the results reported here, led to the hypothesis that the metabolism of ritonavir inhibits CYP3A4 by the formation of a covalent adduct to the apoprotein of CYP3A4.

Covalent labeling of CYP apoprotein has been shown to be the cause of inactivation for a structurally diverse set of compounds including terminal acetylenes such as 1-ethynylpyrene (Gan et al., 1984), furan-containing compounds such as furafylline (Racha et al., 1998), 8-methoxypsoralen (Labbe et al., 1989) and bergamottin (He et al., 1998) and halogenated compounds such as chloramphenicol (Halpert, 1982). The identification of CYP3A4 apo adducts

Molecular Pharmacology Fast Forward. Published on October 1, 2014 as DOI: 10.1124/mol.114.094862
This article has not been copyedited and formatted. The final version may differ from this version.

and the chemical entities responsible for inactivating CYP3A4 are commonly inferred through the identification of glutathione adducts from the incubation medium. The utility of this strategy was confirmed with the mechanism-based inhibitor raloxifene and CYP3A4, whereby one of the reactive metabolites trapped with glutathione was also identified as the perpetrator of CYP3A4 inactivation mediated by raloxifene(Baer et al., 2007). Unfortunately, *in vitro* studies designed to trap electrophilic intermediates from ritonavir bioactivation could not be detected by radiometric LC or LC/MS/MS from incubations with multiple trapping agents, which included glutathione (soft nucleophile) and cyanide (hard nucleophile). More so, co-incubations with these trapping agents had no effect on either the rate of inactivation by ritonavir or on the metabolite profile of ritonavir.

To characterize the potential for ritonavir electrophilic intermediate(s) to form adducts with CYP apoprotein, [^{3}H]-ritonavir, ritonavir and d_6-ritonavir were employed. Historically, radiolabeled material traced the adducted protein through numerous steps including, dialysis, enzymatic digestion and LC/MS to facilitate the location of protein adducts (Racha et al., 1998; Lightning et al., 2000) (Lightning et al., 2000). Given the inability to trap electrophilic intermediates of ritonavir with surrogate nucleophiles, it is suggestive that covalent binding of [^{3}H]-ritonavir electrophiles to CYP3A4 should be proportional to the amount of enzyme in the incubations. These findings were confirmed in incubations with [^{3}H]-ritonavir and CYP3A4 Supersomes™, and in HLMs where the average binding stoichiometry of 0.93 ±0.04 moles of ritonavir bound per mole of CYP3A4 inactivated. More so, the metabolism of [^{3}H]-ritonavir by purified CYP3A4 reconstituted with CYP reductase and cytochrome b_5 lead to the formation of a covalent adduct specifically to CYP3A4 detected by radiometric LC trace.

LC/MS analysis of intact CYP apoprotein adduction provides a complimentary approach to covalent binding data and a direct method to identify irreversible binding of an electrophile in addition to providing a change in mass associated with the adduct. The direct measurement of

Molecular Pharmacology Fast Forward. Published on October 1, 2014 as DOI: 10.1124/mol.114.094862
This article has not been copyedited and formatted. The final version may differ from this version.

the mechanism-based inhibitor offers a distinct advantage over predictions based solely on the identity of a GSH-drug adduct that may or may not be related to the reactive species responsible for the mechanism of CYP inactivation. Whole protein mass spectrometry was utilized to determine if adduction to CYP3A4 occurred and could be detected for ritonavir. Using d_6-ritonavir a whole protein adduct consistent with the oxidized form of ritonavir bound plus six daltons was also observed (data not shown). Enzymatic digestion of the CYP3A4-[^{3}H]-ritonavir incubations exhibited an adducted lysine residue 257 in the peptide 255-RM**K**ESRLEDTQKD-268, associated with a radiochromatic peak and a mass consistent with ritonavir plus 16 daltons, in agreement with the whole protein mass spectroscopy. Given the prevalence of lysine residues in CYP3A protein and the identification of a single lysine-ritonavir adduct, it is hypothesized that lysine 257 is located in an egress channel of CYP3A4 and may adduct other electrophilic-intermediates. Of note, LC/MS/MS data from trypically digested CYP3A4 after incubation routinely yielded sequence coverage above 70% from which a single adducted peptide appeared to be alkylated. These findings were consistent with the LC/MS of intact protein and the use of radiolabled ritonavir in combination with digestion. Collectively, these data conclusively demonstrate that CYP3A4 apoprotein is alkylated by a reactive intermediate formed by the metabolism of ritonavir.

A series of studies were conducted to investigate the mechanism of ritonavir bioactivation and to identify the structure of the covalent adduct to CYP3A4 protein. The two thiazole rings (2'-isopropyl-thiazole and unsubstituted thiazole ring) were considered to be the likely sites of bioactivation based on a comparison of the inhibitory potencies of ritonavir and structural analogs (Kempf et al., 1997). The results suggest that the potent inhibitory properties of ritonavir may require the presence of both thiazole rings in the molecule (Kumar et al., 1996). The literature on the CYP catalyzed bioactivation and metabolism thiazole rings is limited; however, the findings are highly relevant and provide insight into potential mechanisms for

Molecular Pharmacology Fast Forward. Published on October 1, 2014 as DOI: 10.1124/mol.114.094862
This article has not been copyedited and formatted. The final version may differ from this version.

ritonavir inactivation of CYP3A4. Thiazoles are known to undergo CYP-catalyzed oxidative ring opening. For example, Mizutami and co-workers (Mizutani et al., 1994) have demonstrated that ring cleavage of substituted thiazoles results in the formation of the corresponding dicarbonyl metabolites and thioamide derivatives. Conversely, no ring-opened products have been observed in studies reported here and in extensive metabolite ID studies reported elsewhere with ritonavir(Kumar et al., 1996; Denissen et al., 1997; Koudriakova et al., 1998). Finally, substituents in the 4' and 5'-position of the thiazole ring confer resistance to oxidative ring opening, as is the case with ritonavir.

More recently, two studies have reported that cytochrome CYPs can catalyze the bioactivation of thiazole rings to intermediates that form covalent bonds to protein (Subramanian et al.; Obach et al., 2008) via the formation of an epoxide intermediate. The structures of the GSH adducts to bioactivated thiazoles (e.g sudoxicam, meloxicam and multiple 2-aminothiazole derivatives) have been determined. Thiazole ring bioactivation is proposed to occur as the result of oxidation of the thiazole ring to a reactive epoxide. The formation of this epoxide is highly dependent on the position of the substitutes on the thiazole ring. Subramanian and co-workers (Subramanian et al.) examined the metabolism of a library of variously substituted thiazole rings. In most cases, it was concluded that substitution at the 3'-position on the thiazole ring abolishes both epoxide formation and subsequent GSH adduct formation. Therefore, if epoxidation of ritonavir does occur, the most probable site of oxygen attack is on the unsubstituted thiazole ring. The results of the proteinase K digestion suggest that ritonavir is bioactivated at the opposite end of the molecule from the unsubsititued thiazole ring. Therefore, we propose the route of inactivation is most likely via a sulfoxide intermediate, followed by nucleophilic attack by the lysine residue (Scheme 1, pathway B).

In conclusion, ritonavir exhibited potent time-dependent inactivation of CYP3A, by which the mechanism of inactivation was through a covalent bond to Lys257 of the CYP3A4

Molecular Pharmacology Fast Forward. Published on October 1, 2014 as DOI: 10.1124/mol.114.094862
This article has not been copyedited and formatted. The final version may differ from this version.

apoprotein. Metabolism studies and inhibition profiles helped to eliminate heme adduction and MI complex by ritonavir and lead to the conclusion that CYP3A4 inactivation by ritonavir occurs via a covalent bond to the apoprotein. Intact whole protein mass spectroscopy was crucial to determine the mechanism of inactivation given the lack of a ritonavir adduct to any exdogenous trapping agents. However, the exact structure of the bioactivated ritonavir bound to the lysine residue remains unclear. Therefore, further investigation into the reactivity of thiazole rings and cytochrome CYP enzymes may provide further insights into the reactive intermediate structure as well as the interactions between CYP 3A4 and reactive intermediate formation.

Molecular Pharmacology Fast Forward. Published on October 1, 2014 as DOI: 10.1124/mol.114.094862
This article has not been copyedited and formatted. The final version may differ from this version.

Authorship Contributions

Participated in research design: B.Rock, Hengel, D.Rock, Wienkers and Kunze

Conducted experiments: B.Rock D.Rock

Contributed new reagents or analytic tools: none

Performed data analysis: B.Rock, D.Rock

Wrote or contributed to the writing of the manuscript: B.Rock and Kunze

References:

Baer BR, Wienkers LC, and Rock DA (2007) Time-dependent inactivation of P450 3A4 by raloxifene: identification of Cys239 as the site of apoprotein alkylation. *Chem Res Toxicol* **20:**954-964. Epub 2007 May 2012.

Begriche K, Massart J, Robin MA, Borgne-Sanchez A, and Fromenty B (2011) Drug-induced toxicity on mitochondria and lipid metabolism: Mechanistic diversity and deleterious consequences for the liver. *J Hepatol* **54:**773-794.

Bensoussan C, Delaforge M, and Mansuy D (1995) Particular ability of cytochrome P450 3A to form inhibitory P450-iron-metabolite complexes upon metabolic oxidation of aminodrugs. *Biochem Pharmacol* **49:**591-602.

Blobaum AL, Kent UM, Alworth WL, and Hollenberg PF (2002) Mechanism-based inactivation of cytochromes P450 2E1 and 2E1 T303A by tert-butyl acetylenes: characterization of reactive intermediate adducts to the heme and apoprotein. *Chem Res Toxicol* **15:**1561-1571.

Delaforge M, Jaouen M, and Mansuy D (1984) The cytochrome P-450 metabolite complex derived from troleandomycin: properties in vitro and stability in vivo. *Chem Biol Interact* **51:**371-376.

Denissen JF, Grabowski BA, Johnson MK, Buko AM, Kempf DJ, Thomas SB, and Surber BW (1997) Metabolism and disposition of the HIV-1 protease inhibitor ritonavir (ABT-538) in rats, dogs, and humans. *Drug Metab Dispos* **25:**489-501.

Ernest CS, 2nd, Hall SD, and Jones DR (2005) Mechanism-based inactivation of CYP3A by HIV protease inhibitors. *J Pharmacol Exp Ther* **312:**583-591.

Fernandez-Montero JV, Barreiro P, and Soriano V (2009) HIV protease inhibitors: recent clinical trials and recommendations on use. *Expert Opin Pharmacother***:**1615-1629.

Fletcher CV, Acosta EP, Cheng H, Haubrich R, Fischl M, Raasch R, Mills C, Hu XJ, Katzenstein D, Remmel RP, and Gulick RM (2000) Competing drug-drug interactions among multidrug antiretroviral regimens used in the treatment of HIV- infected subjects: ACTG 884. *Aids* **14:**2495-2501.

Gan LS, Acebo AL, and Alworth WL (1984) 1-Ethynylpyrene, a suicide inhibitor of cytochrome P-450 dependent benzo[a]pyrene hydroxylase activity in liver microsomes. *Biochemistry* **23:**3827-3836.

Halpert J (1982) Further studies of the suicide inactivation of purified rat liver cytochrome P-450 by chloramphenicol. *Mol Pharmacol* **21:**166-172.

He K, Iyer KR, Hayes RN, Sinz MW, Woolf TF, and Hollenberg PF (1998) Inactivation of cytochrome P450 3A4 by bergamottin, a component of grapefruit juice. *Chem Res Toxicol* **11:**252-259.

Hirsch MS, Gunthard HF, Schapiro JM, Brun-Vezinet F, Clotet B, Hammer SM, Johnson VA, Kuritzkes DR, Mellors JW, Pillay D, Yeni PG, Jacobsen DM, and Richman DD (2008) Antiretroviral drug resistance testing in adult HIV-1 infection: 2008 recommendations of an International AIDS Society-USA panel. *Top HIV Med* **16:**266-285.

Kempf DJ, Marsh KC, Kumar G, Rodrigues AD, Denissen JF, McDonald E, Kukulka MJ, Hsu A, Granneman GR, Baroldi PA, Sun E, Pizzuti D, Plattner JJ, Norbeck DW, and Leonard JM (1997) Pharmacokinetic enhancement of inhibitors of the human immunodeficiency virus protease by coadministration with ritonavir. *Antimicrob Agents Chemother* **41:**654-660.

Koudriakova T, Iatsimirskaia E, Utkin I, Gangl E, Vouros P, Storozhuk E, Orza D, Marinina J, and Gerber N (1998) Metabolism of the human immunodeficiency virus protease inhibitors indinavir and ritonavir by human intestinal microsomes and expressed cytochrome P4503A4/3A5: mechanism-based inactivation of cytochrome P4503A by ritonavir. *Drug Metab Dispos* **26:**552-561.

Kumar GN, Rodrigues AD, Buko AM, and Denissen JF (1996) Cytochrome P450-mediated metabolism of the HIV-1 protease inhibitor ritonavir (ABT-538) in human liver microsomes. *J Pharmacol Exp Ther* **277:**423-431.

Kunze KL, Mangold BL, Wheeler C, Beilan HS, and Ortiz de Montellano PR (1983) The cytochrome P-450 active site. Regiospecificity of prosthetic heme alkylation by olefins and acetylenes. *J Biol Chem* **258:**4202-4207.

Labbe G, Descatoire V, Beaune P, Letteron P, Larrey D, and Pessayre D (1989) Suicide inactivation of cytochrome P-450 by methoxsalen. Evidence for the covalent binding of a reactive intermediate to the protein moiety. *J Pharmacol Exp Ther* **250:**1034-1042.

Lightning LK, Jones JP, Friedberg T, Pritchard MP, Shou M, Rushmore TH, and Trager WF (2000) Mechanism-based inactivation of cytochrome P450 3A4 by L-754,394. *Biochemistry* **39:**4276-4287.

Lin HL, D'Agostino J, Kenaan C, Calinski D, and Hollenberg PF (2013) The effect of ritonavir on human CYP2B6 catalytic activity: heme modification contributes to the mechanism-based inactivation of CYP2B6 and CYP3A4 by ritonavir. *Drug Metab Dispos* **41:**1813-1824. doi: 1810.1124/dmd.1113.053108. Epub 052013 Jul 053125.

Lin HL and Hollenberg PF (2007) The inactivation of cytochrome P450 3A5 by 17alpha-ethynylestradiol is cytochrome b5-dependent: metabolic activation of the ethynyl moiety leads to the formation of glutathione conjugates, a heme adduct, and covalent binding to the apoprotein. *J Pharmacol Exp Ther* **321:**276-287.

Liu Z and Franklin MR (1985) Cytochrome P-450 ligands: metyrapone revisited. *Arch Biochem Biophys* **241:**397-402.

Mayhew BS, Jones, D. R., Hall, S. D. (2000) An In Vitro Model for Predicting In Vivo Inhibition of Cytochrome P450 3A4 by Metabolic Intermediate Complex Formation. *Drug Metabolism and Disposition* **28:**1031-1037.

Miller CD, El-Kholi R, Faragon JJ, and Lodise TP (2007) Prevalence and risk factors for clinically significant drug interactions with antiretroviral therapy. *Pharmacotherapy* **27:**1379-1386.

Mizutani T, Yoshida K, and Kawazoe S (1994) Formation of toxic metabolites from thiabendazole and other thiazoles in mice. Identification of thioamides as ring cleavage products. *Drug Metab Dispos* **22:**750-755.

Moyle GJ and Back D (2001) Principles and practice of HIV-protease inhibitor pharmacoenhancement. *HIV Med* **2:**105-113.

Obach RS, Kalgutkar AS, Ryder TF, and Walker GS (2008) In vitro metabolism and covalent binding of enol-carboxamide derivatives and anti-inflammatory agents sudoxicam and meloxicam: insights into the hepatotoxicity of sudoxicam. *Chem Res Toxicol* **21:**1890-1899.

Ortiz de Montellano PR (2005) *Cytochrome P450: Structure, Mechanism, and Biochemistry*. Kluwer Academic/Plenum Publishers, New York.

Ortiz de Montellano PR and Kunze KL (1981) Cytochrome P-450 inactivation: structure of the prosthetic heme adduct with propyne. *Biochemistry* **20:**7266-7271.

Racha JK, Rettie AE, and Kunze KL (1998) Mechanism-based inactivation of human cytochrome P450 1A2 by furafylline: detection of a 1:1 adduct to protein and evidence for the formation of a novel imidazomethide intermediate. *Biochemistry* **37:**7407-7419.

Schenkman JB, Wilson BJ, and Cinti DL (1972) Dimethylaminoethyl 2,2-diphenylvalerate HCl (SKF 525-A)--in vivo and in vitro effects of metabolism by rat liver microsomes--formation of an oxygenated complex. *Biochem Pharmacol* **21:**2373-2383.

Sevrioukova IF and Poulos TL (2010) Structure and mechanism of the complex between cytochrome P4503A4 and ritonavir. *Proc Natl Acad Sci U S A* **107:**18422-18427.

Shaw PM, Hosea NA, Thompson DV, Lenius JM, and Guengerich FP (1997) Reconstitution premixes for assays using purified recombinant human cytochrome P450, NADPH-cytochrome P450 reductase, and cytochrome b5. *Arch Biochem Biophys* **348:**107-115.

Silverman RB (1988) *Mechanism-based Enzyme Inactivation: Chemistry and Enzymology*. CRC Press.

Subramanian R, Lee MR, Allen JG, Bourbeau MP, Fotsch C, Hong FT, Tadesse S, Yao G, Yuan CC, Surapaneni S, Skiles GL, Wang X, Wohlhieter GE, Zeng Q, Zhou Y, Zhu X, and Li C Cytochrome P450-Mediated Epoxidation of 2-Aminothiazole-Based AKT Inhibitors: Identification of Novel GSH Adducts and Reduction of Metabolic Activation through Structural Changes Guided by in Silico and in Vitro Screening. *Chem Res Toxicol*.

Takakusa H, Wahlin MD, Zhao C, Hanson KL, New LS, Chan EC, and Nelson SD (2011) Metabolic intermediate complex formation of human cytochrome P450 3A4 by lapatinib. *Drug Metab Dispos* **39:**1022-1030.

Yates JR, 3rd, Eng JK, McCormack AL, and Schieltz D (1995) Method to correlate tandem mass spectra of modified peptides to amino acid sequences in the protein database. *Anal Chem* **67:**1426-1436.

Molecular Pharmacology Fast Forward. Published on October 1, 2014 as DOI: 10.1124/mol.114.094862
This article has not been copyedited and formatted. The final version may differ from this version.

Scheme Legends

Scheme 1. Metabolic pathways proposed for the formation of reactive intermediate of ritonavir responsible for covalently modifying CYP 3A4 leading to inactivation of the enzyme

Figure Legends

Figure 1. Chemical structures of ritonavir (A) and a primary metabolite of ritonavir, N-ritonavir. *Indicated the [^{3}H]-label on ritonavir.

Figure 2. (A) Percentage of MI complex formed calculated by the extinct coefficient of 65 mM^{-1} cm^{-1} and compared to theoretical maximum, where 10 µM N-Ritonavir (solid circles), 10 µM N-Ritonavir + 1 µM Ritonavir (open down triangles), 10 µM N-Ritonavir + 10 µM Ritonavir (solid squares) and 10 µM Ritonavir (open up triangles). (B) 1 mM potassium ferricyanide ($K_3[Fe(CN)_6]$) was added to incubations containing CYP3A4 and 10 µM Ritonavir (RTV), N-Ritonavir (N-RTV) or troleandomyocin (TAO), a positive control (striped bars). Enzyme activity was determined before (control, open bars) and after ferricyanide addition in secondary assays using midazolam as the substrate. Return of activity to normal levels was observed for TAO and N-RTV, but not RTV. (C) Final MI complex spectra obtained by incubation of each compound with 0.1 µM P450 3A4. MI complex formation by 10 µM N-ritonavir (——), 10 µM N-Ritonavir + 1 µM Ritonavir (– – –), 10 µM N-Ritonavir + 10 µM Ritonavir (· · · · ·) and 10 µM Ritonavir (——).. The absorption (ABS) maximum for each complex ranged was 455 nm. Scans were recorded for 15 min total (20-s intervals).

Figure 3. Effect of ritonavir inactivation on the reduced CO difference spectrum of CYP3A4. The reduced CO difference spectra of CYP3A4 in the reconstituted system incubated with 10 µM

ritonavir in the absence (solid line) or presence (dashed line) of NADPH for 30 min were measured. A posttive control, 1-Aminobenzotriazole, is shown in dotted line.

Figure 4. [^{3}H]-Ritonavir(1.5 μM) was incubated (± NADPH) with CYP3A4 reconstituted with cytochrome b_5 and P450 reductase. Incubations were analyzed by UV-HPLC at 220 nm (A), and radiometric-LC (B). Based on injection of standards, the elution times were heme (a, 18 min), cytochrome b_5 (b, 24 min), P450 reductase (c, 26 min) and CYP3A4 (d, 28 min). Minus NADPH samples had no detectable amounts of radioactivity.

Figure 5. (A)1.5 uM of [^{3}H]-RTV was incubated with CYP3A4 supersomes™ as well as three separate lots (144, 160 and 169) of HLMs for 60 min in the presence and absence of NADPH. the protein was precipiated after addition of H_2SO_4/methanol, centrifuged and washed repeatedly to background. Covalently bound radioactivity [^{3}H]-RTV was converted to RTV equivalents expressed in pmoles. (B) the linear correlation of bound pmoles of [^{3}H]-RTV to amount of CYP3A with a slope of 0.93.

Figure 6. LC-MS deconvoluted spectra for P450 3A4 incubations where (A) minus NADPH, plus ritonavir and (B) plus NADPH, plus ritonavir.

Figure 7. MS/MS spectra of the CYP3A4 ritonavir-adducted peptide, 255-RMkESRLEDTQKHR-268. Spectrum acquired at 23.5 min with parent $[M+2H]^{2+}$ = *m/z* 1276.1329. Blue ions (y ions) and red ions (b ions) masses are listed in the table. The peak labeled *m/z* = 749.12 corresponds to ritonavir (+16 daltons) attached to a nitrogen, presumably from lysine 257

Molecular Pharmacology Fast Forward. Published on October 1, 2014 as DOI: 10.1124/mol.114.094862
This article has not been copyedited and formatted. The final version may differ from this version.

Tables

Table 1. Kinetic parameters of inactivation for P450 3A4 by ritonavir and a primary metabolite, N-ritonavir

	K_I	k_{inact}	Partition Ratio
Ritonavir	0.59 ±0.12 μM	0.53 ±0.05 min^{-1}	19 ±3
N-ritonavir	1.4 ±0.3 μM	0.33 ±0.2 min^{-1}	12 ±2

Scheme 1

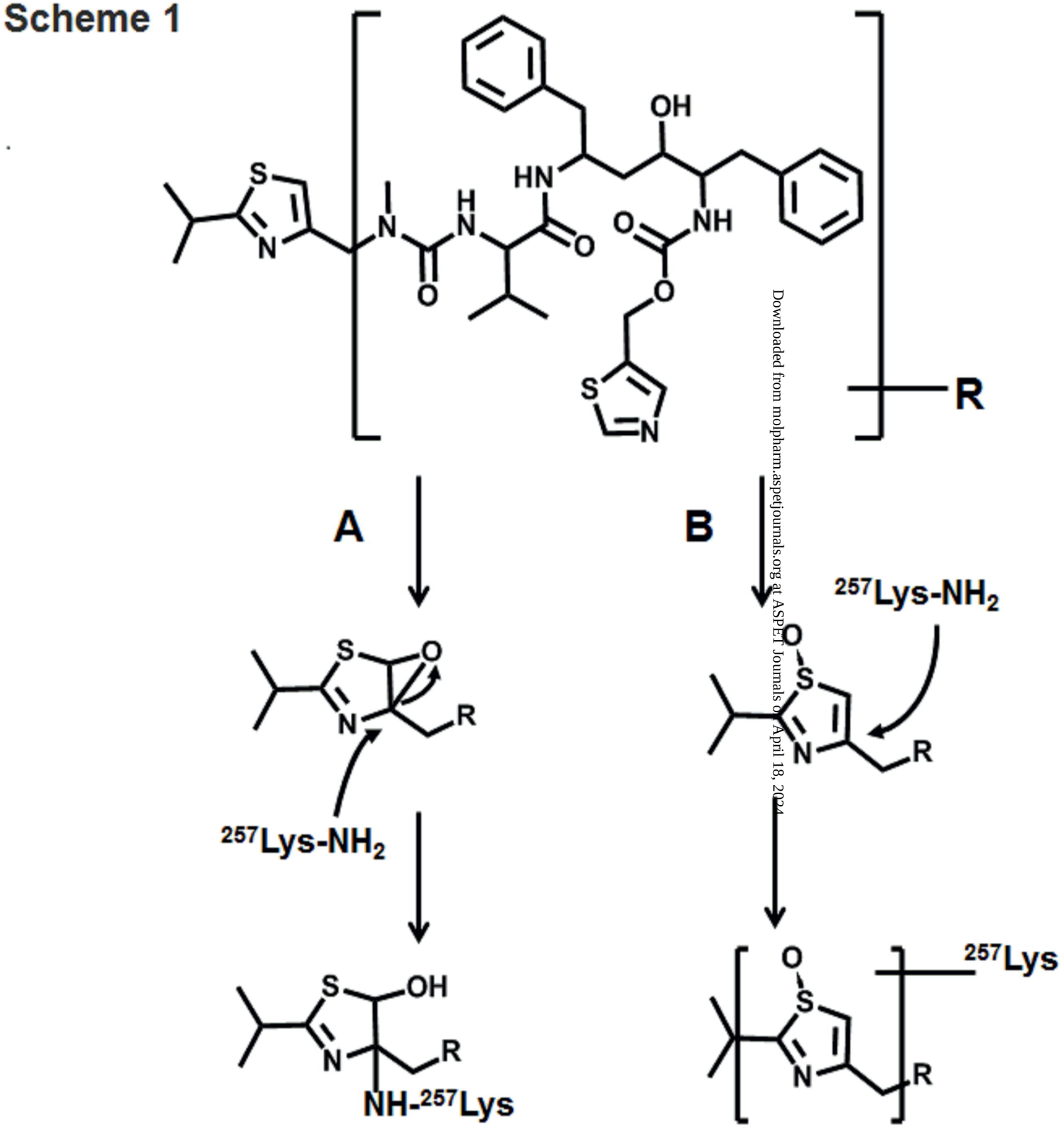

Figure 1

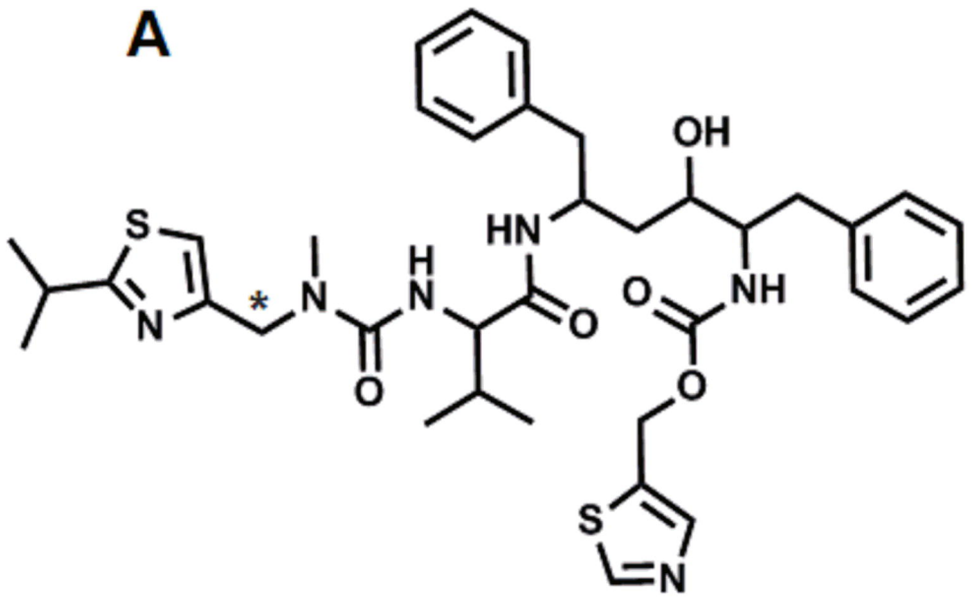

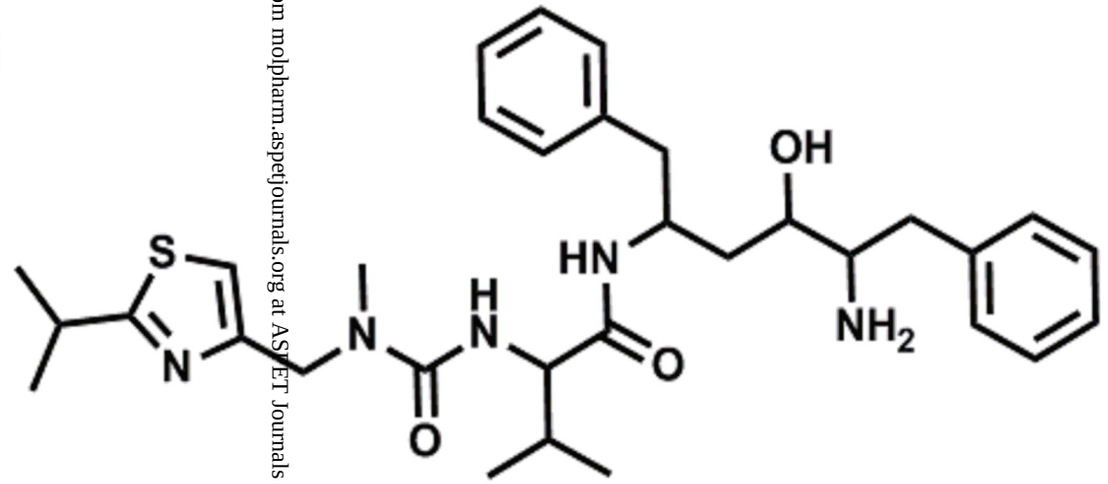

Molecular Pharmacology Fast Forward. Published on October 1, 2014 as DOI: 10.1124/mol.114.094862

Figure 2

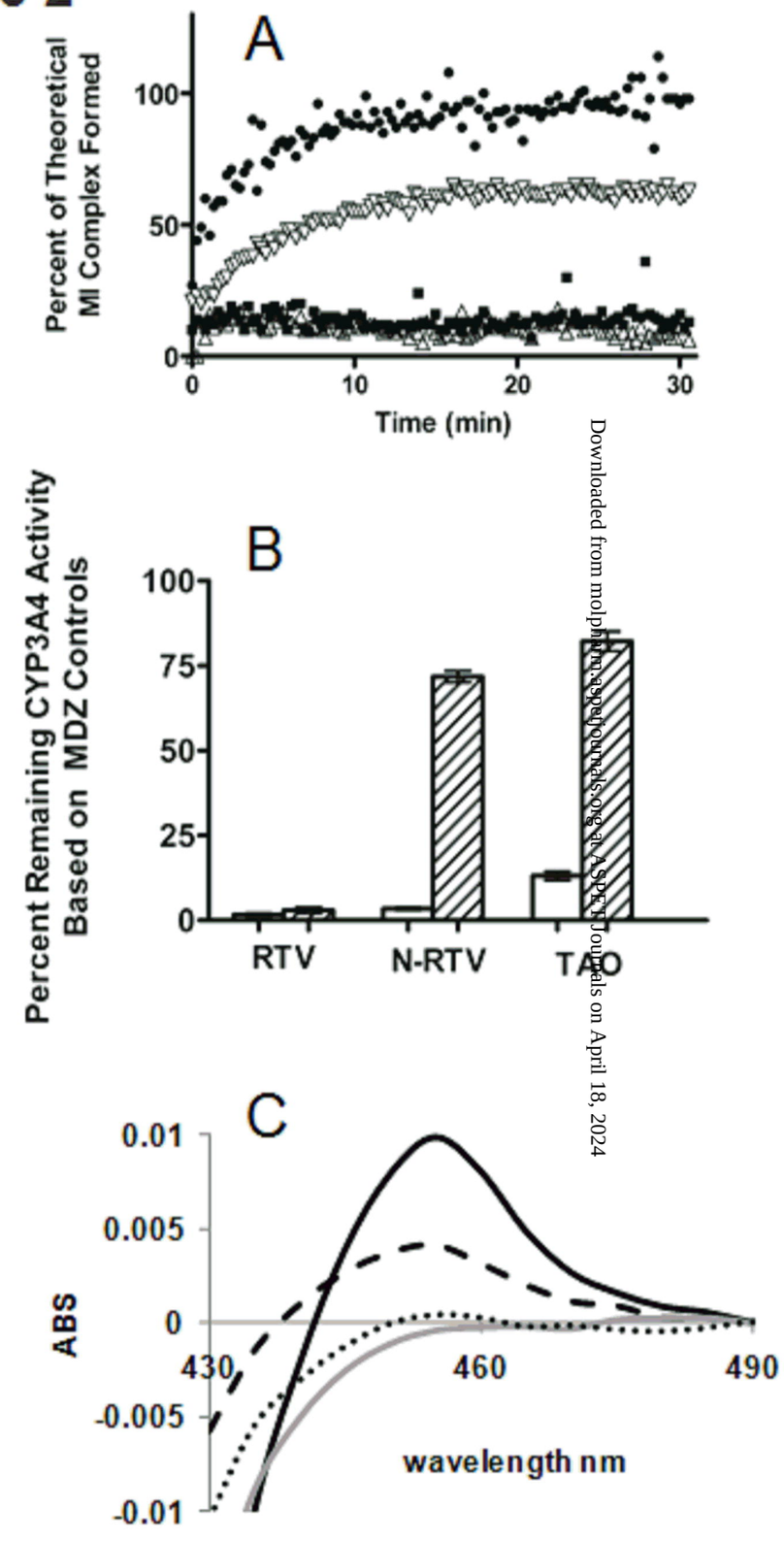

Figure 3

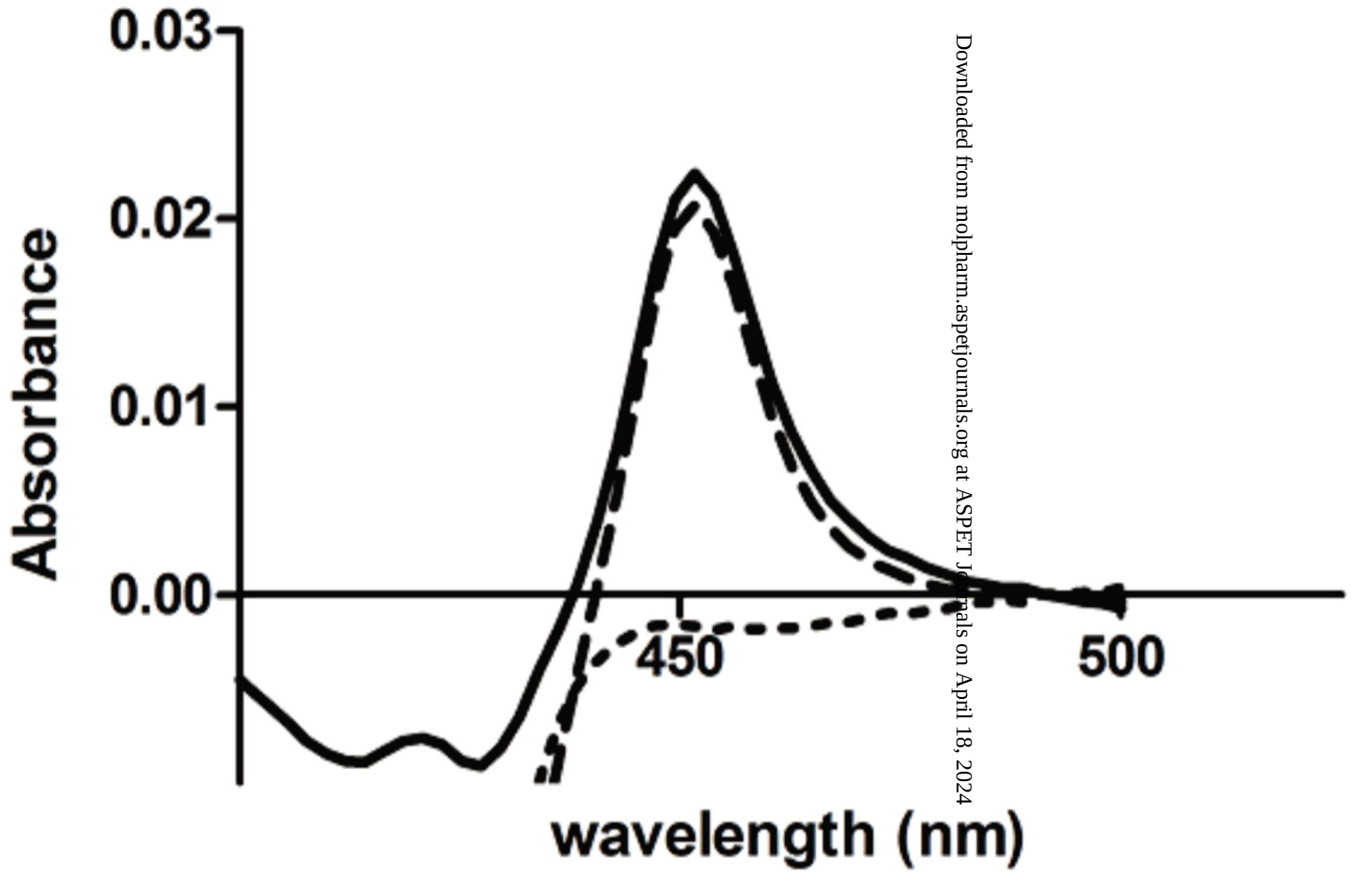

Molecular Pharmacology Fast Forward. Published on October 1, 2014 as DOI: 10.1124/mol.114.094862
This article has not been copyedited and formatted. The final version may differ from this version.

Figure 4

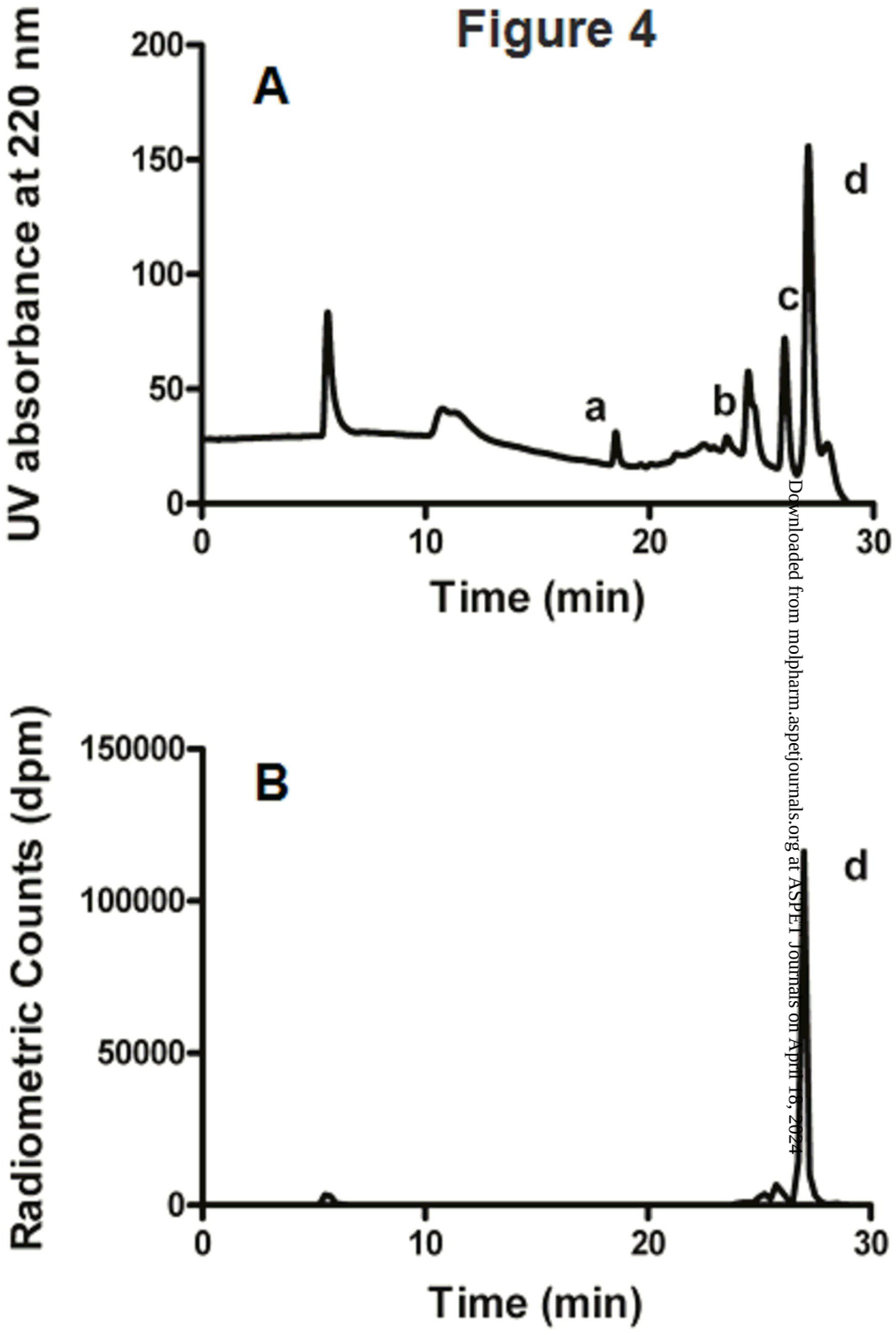

Figure 5

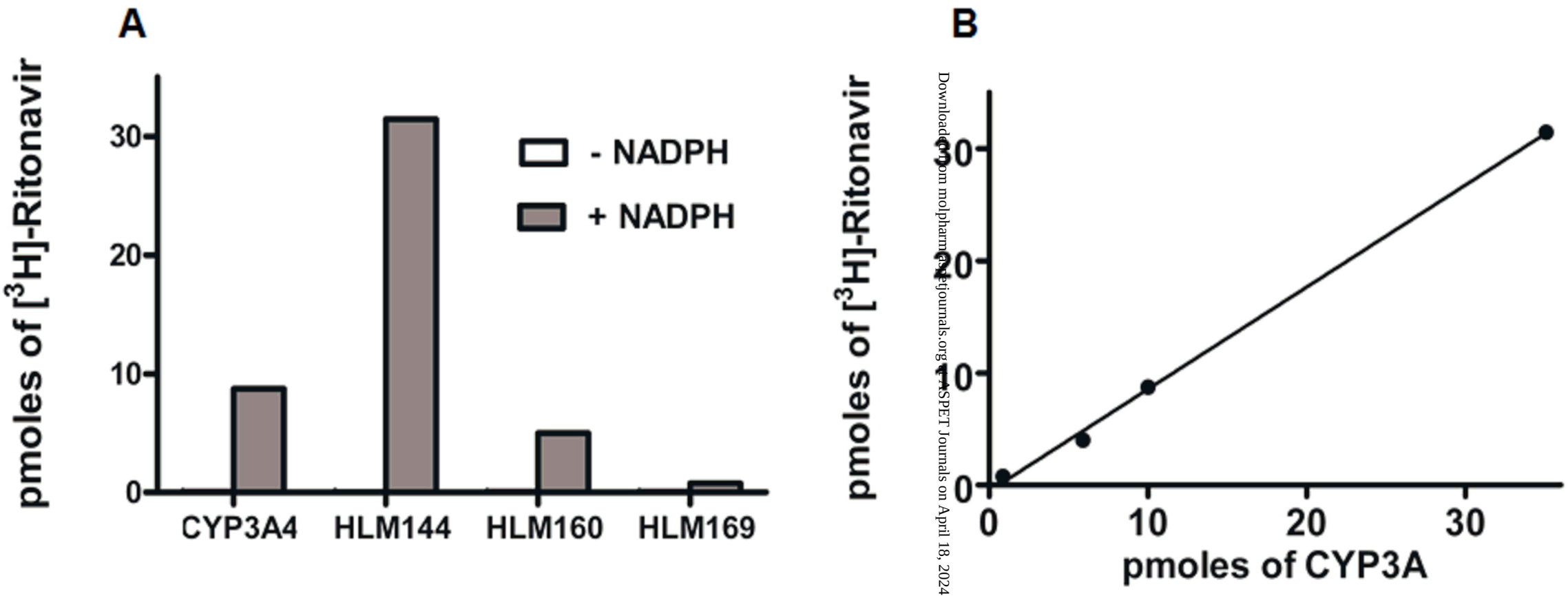

Figure 6

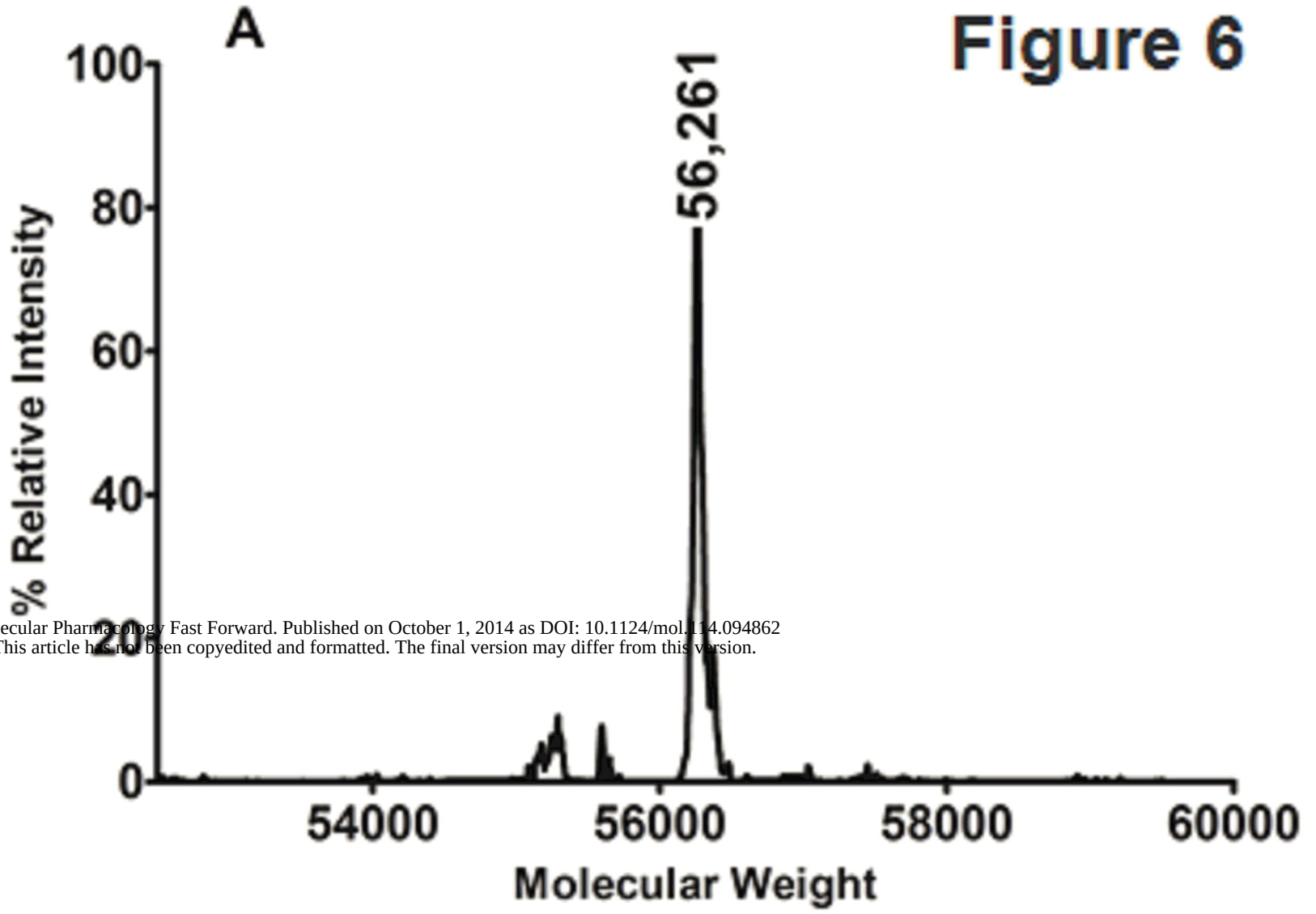

Figure 7

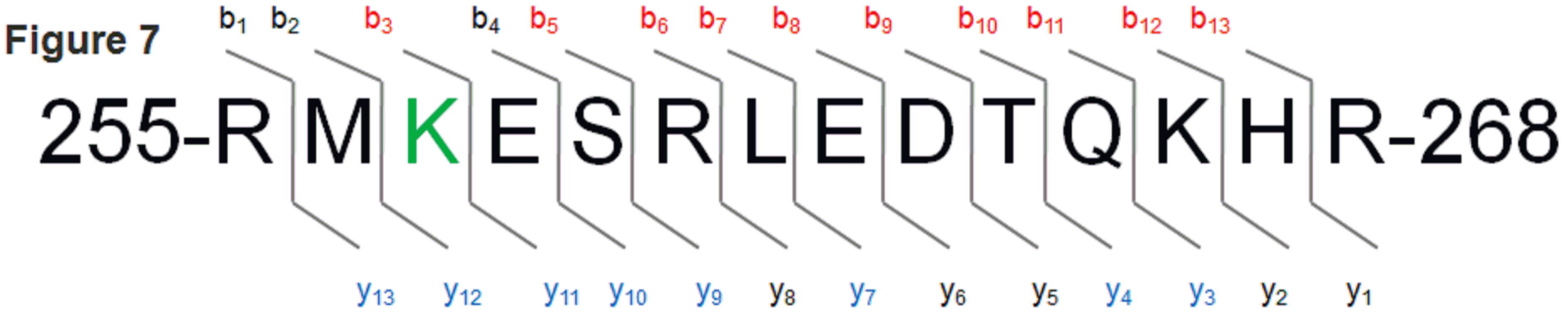

b^+	b^{2+}		y^+	y^{2+}
157.10840	79.05784	R		
288.14890	144.57809	M	2393.14374	1197.07551
1151.54367	576.27547	K*	2262.10324	1131.55526
1280.58627	640.79677	E	1398.70847	699.85787
1367.61830	684.31279	S	1269.66587	635.33657
1523.71942	762.36335	R	1182.63384	591.82056
1636.80349	818.90538	L	1026.53272	513.77000
1765.84609	883.42668	E	913.44865	457.22796
1880.87304	940.94016	D	784.40605	392.70666
1981.92072	991.46400	T	669.37910	335.19319
2109.97930	1055.49329	Q	568.33142	284.66935
2238.07427	1119.54077	K	440.27284	220.64006
2375.13318	1188.07023	H	312.17787	156.59257
		R	175.11896	88.06312